

Silicide structural evolution in high-dose cobalt-implanted Si(100) crystals

Zheng-quan Tan, J. I. Budnick, and F. H. Sanchez*

Department of Physics and Institute of Materials Science, University of Connecticut, Storrs, Connecticut 06269-3046

G. Tourillon

Laboratoire pour l'Utilisation du Rayonnement Electromagnétique, Bâtiment 209D, 91405 Orsay CEDEX, France

F. Namavar[†] and H. C. Hayden

Department of Physics and Institute of Materials Science, University of Connecticut, Storrs, Connecticut 06269-3046

(Received 4 April 1989; revised manuscript received 5 June 1989)

The silicide structure in high-dose $[(1-8) \times 10^{17} \text{ Co/cm}^2]$ cobalt-implanted Si(100) crystals is studied by extended x-ray-absorption fine structure, x-ray diffraction, and Rutherford backscattering spectrometry. As the implant dose increases we observe silicide structural evolution from a locally ordered CoSi_2 at a dose of $1 \times 10^{17} \text{ Co/cm}^2$, to long-range-ordered CoSi_2 and CoSi at $3 \times 10^{17} \text{ Co/cm}^2$, and to a short-range-ordered and highly defective CoSi -like structure at $8 \times 10^{17} \text{ Co/cm}^2$. We propose a model in which Co atoms preferentially occupy the interstitial site, first in silicon then in CoSi_2 , to understand the silicide-formation mechanism in the implanted system. The short-range-ordered silicides, observed for the first time, and the structural evolution are discussed in terms of both the CoSi_2 and CoSi structures and the proposed model. Single-phase and strongly oriented CoSi_2 are obtained in samples annealed at 700°C .

I. INTRODUCTION

There has been growing interest in producing metal silicides by high-dose ion implantation into silicon.¹⁻⁵ The implantation may serve as an alternative and in some aspects advantageous method to other deposition methods in the fabrication of circuit-device-oriented materials. CoSi_2 and NiSi_2 have attracted particular attention because of their superior electrical properties (e.g., low resistivity⁶) and the feasibility of epitaxial growth with silicon. From the few cases studied to date, metal silicide formation produced by implantation has shown rich phenomenology that differs from solid-state reaction of sequentially deposited layers. For example, silicon-rich silicides form readily in the implanted system at quite low substrate temperatures (Refs. 4 and 5 and this work), while in the case of deposited layers they form only at much higher temperatures and often after metal-rich silicides are formed.^{7,8} The understanding of the silicide formation process in the implanted system is of fundamental value and will be beneficial to achieving high-quality materials, but to date, such understanding is very limited. We report here a detailed study of the silicide structure of high-dose cobalt-implanted systems. We have utilized extended x-ray-absorption fine structure (EXAFS) capable of probing short-range structural order, and x-ray diffraction which probes long-range ordered phases. EXAFS with its element selectivity and short-range sensitivity is ideal for revealing the local environment of the im-

planted species. Composition profiles are obtained with Rutherford backscattering spectrometry (RBS).

II. EXPERIMENT

Polished single-crystal silicon with (100) orientation was uniformly implanted using a scanning beam of 150-keV and 165-keV Co^+ ions at substrate temperatures between 100 and 400°C in a vacuum of 10^{-6} Torr. Current densities of $10-20 \mu\text{A/cm}^2$ were used to achieve total doses of $(1-8) \times 10^{17} \text{ Co/cm}^2$. The sample holder was surrounded by a liquid-nitrogen trap and warmed by a heater with temperature monitored and stabilized during the implantation. Further description of the implantation apparatus has appeared elsewhere.⁹ The EXAFS measurements were carried out at Beam Line X-11 at the National Synchrotron Light Source (NSLS) and at Laboratoire pour l'Utilisation du Rayonnement Electromagnétique (LURE) in France. At X-11 a Si(111) double-crystal monochromator with a 0.5-mm front slit was used and the energy resolution at the Co *K* edge was estimated to be 2.5 eV. Harmonics were rejected by detuning the crystals to cut 20% of the peaked incident intensity. Implanted samples were measured by fluorescence detection with 45° incidence and 45° exit set up plus an Fe filter with slit assembly.¹⁰ Such a setup turns out to be quite effective in eliminating the diffraction peaks from the Si(100) substrate. Data on CoSi_2 , FeSi , and cobalt foil were measured in transmission. Electron-yield detection¹¹ of EXAFS was used in measurements carried out

at LURE. The purity and structure of the commercially obtained CoSi_2 and FeSi were checked with x-ray-diffraction measurements.

III. RESULTS

A. RBS and x-ray diffraction

The cobalt-implanted samples were characterized by RBS measurements with a 1.9-MeV ^4He beam. The RBS spectra were discussed previously¹² and are summarized here. The Co concentration profile is shown in Fig. 1 for the 1×10^{17} -, 3×10^{17} -, and 8×10^{17} -Co/cm² samples. They show a peak concentration of 12%, 40%, and 44%, respectively. The Co in the 1×10^{17} -Co/cm² sample is buried with a peak at 1000 Å. Co diffusion from the surface region towards the peak Co concentration region is observed after annealing at 700 °C for 2 h (dashed line in Fig. 1). This will be discussed further in the context of CoSi_2 growth upon annealing. For the 3×10^{17} - and 8×10^{17} -Co/cm² samples a large amount of Co appears at the surface and the Co concentration remains more or less constant in the top 1000-Å layer.

Ordered silicides in most of the implanted samples observed by XRD are preferentially oriented. For the as-implanted samples, only a few weak lines that can be indexed with the orthorhombic Co_2Si structure were observed in the 1×10^{17} -Co/cm² sample. CoSi and a majority CoSi_2 with complete (400) orientation are found in the 3×10^{17} -Co/cm² sample. In the 8×10^{17} -Co/cm² sample only one weak and broad line that can be associated with CoSi with a lattice parameter expanded by 0.10 ± 0.04 Å is detected. These diffraction measurements are to be compared with the EXAFS results on corresponding samples. After thermal annealing at typically 700 °C for

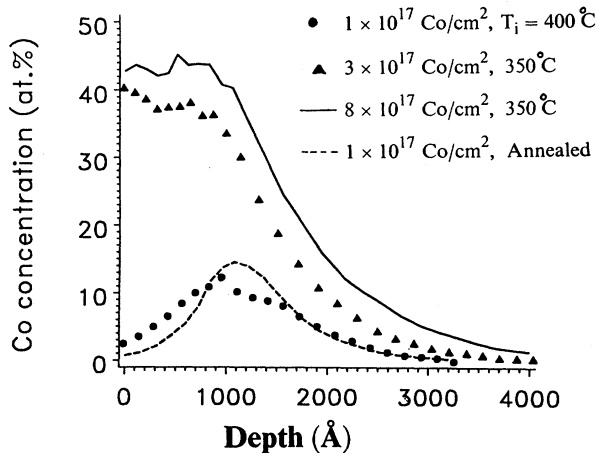


FIG. 1. The Co-atom concentration profile obtained from 1.9-MeV ^4He RBS measurements for cobalt-implanted Si(100) samples with dose and implantation temperature indicated. The 1×10^{17} -Co/cm² sample has also been annealed at 700 °C for two hours. The concentration profiles were obtained by assuming the sample density as a linear combination of the bulk atomic densities of Si and Co; the effects of the energy straggling and the finite detector resolution were not corrected for.

2 h, all implanted samples form single-phase and almost completely oriented $\text{CoSi}_2(400)$. We have proven¹³ that the CoSi_2 in some of our annealed samples is high-quality single-crystal epitaxially grown on the silicon substrate.

B. EXAFS results

The EXAFS refers to the oscillations above an absorption edge in the absorption coefficient. Physically, these oscillations originate from the interference of the outgoing and backscattered (by the near-neighbor atoms) photoelectron wave functions. The EXAFS function for an unoriented sample is given by¹⁴

$$\chi(k) = \sum \frac{N_j S_0^2 F_j(k)}{k R_j^2} e^{-2k^2 \sigma_j^2} e^{-2(R_j - \Delta)/\lambda} \times \sin[2kR_j + \phi_j(k)], \quad (1)$$

where the summation is over coordination shells of a coordination number N_j at an average distance R_j with a mean-squared variance σ_j^2 (MSRD). k is the photoelectron wave vector. $F_j(k)$ is the backscattering amplitude and $\phi_j(k)$ is the total phase shift due to the backscattering atom and the absorber. λ is the mean free path of the photoelectron. S_0^2 accounts for the relaxation effect of the passive electrons, and $\Delta \cong R_1$ compensates for the energy losses included in S_0^2 and $F_j(k)$. The EXAFS data were analyzed with the standard method¹⁵ using CoSi_2 and cobalt metal as reference compounds for Co-Si and Co-Co pairs, respectively. The EXAFS functions obtained after background subtraction were normalized to the step size at the absorption edge.

Fourier-transform magnitudes are presented in Fig. 2 for the as-implanted and annealed 1×10^{17} -Co/cm² sample together with that of bulk CoSi_2 . It is clear that CoSi_2 is formed in both the as-implanted and annealed samples just from comparing their transforms with that of CoSi_2 . The first coordination shell about the Co atom has eight Si atoms at $R = 2.32$ Å (the peak at 2 Å in Fig. 2). From an analysis of log-ratio and nonlinear least-squares fitting of this first-shell data, we find that the CoSi_2 in the annealed sample is well ordered and the near-neighbor distance R , coordination number N , and σ^2 for the first shell are the same, within experimental uncertainties, as those of the bulk CoSi_2 . The result is in good agreement with the XRD results. EXAFS results also show single-phase CoSi_2 in the 3×10^{17} - and 8×10^{17} -Co/cm² samples annealed at 700 °C for two hours. We will concentrate on the as-implanted samples in the following.

No silicide phase other than CoSi_2 is identified by EXAFS in the as-implanted 1×10^{17} -Co/cm² sample. Co-Co pairs in the 2.53–2.67-Å range expected from Co_2Si were not found in the EXAFS data. Therefore, if some Co_2Si exists in the as-implanted sample as suggested by the diffraction measurement, its relative amount should be very small. It is surprising that the predominant CoSi_2 observed in EXAFS is not detected in XRD of the as-implanted sample. There are two possible origins for this. One is that the CoSi_2 grows in the Si(100) wafer ep-

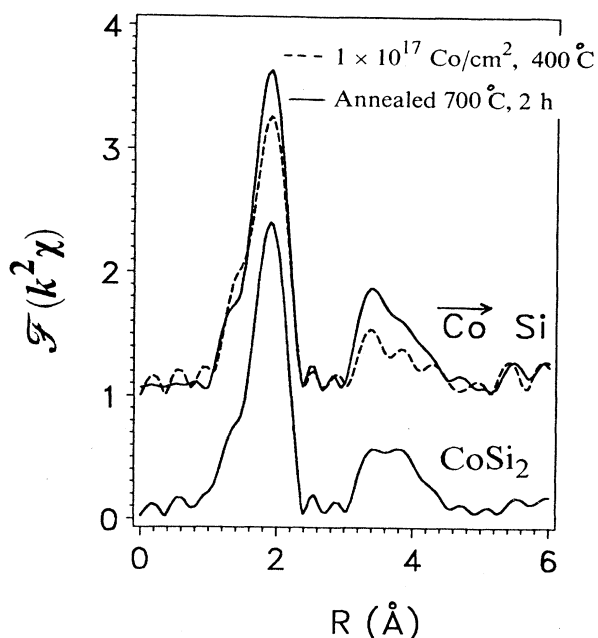


FIG. 2. Fourier-transform magnitude \mathcal{F} of Co EXAFS ($k^2\chi$) for the 1×10^{17} -Co/cm² and $T_i = 400^\circ\text{C}$ samples at room temperature. Dashed line, as-implanted; solid line, annealed at 700°C for two hours. The data for CoSi₂ (lower part) is also included.

itaxially with a perfect match between their lattice parameters such that the only diffraction peak (400) from the CoSi₂ overlaps with the (400) peak from the Si(100) substrate. This epitaxial growth would lead to a Co-Si distance of 2.35 Å, but the Co-Si distance determined in the EXAFS data is $R = 2.32 \pm 0.01$ Å. Thus, such an epitaxial growth appears not to exist in the sample. The remaining origin is that the CoSi₂ is only locally ordered and lacks the long-range order required for the diffraction observation. We point out that the observed local order is compatible with a rather long-range order and high degree of crystallinity within the CoSi₂ grains.

Figure 3 shows the Fourier transform of the EXAFS function for the as-implanted 3×10^{17} -Co/cm² sample. The spectrum is similar to but differs slightly from that of CoSi₂ (see Fig. 2 for CoSi₂ spectrum), suggesting a majority of the CoSi₂ phase and other minority phases. Using the XRD result as a guideline, we have successfully fit the first peak to a combined contribution from 76% CoSi₂ and 24% CoSi, the fit being shown as a dashed line in Fig. 3. Such relative amounts of CoSi₂ and CoSi give an overall Co-atom concentration of 37% in the CoSi₂ and CoSi region neglecting possible unreacted silicon in this region. The close match of this value with that obtained by RBS profile (Fig. 1) seems to suggest the existence of a silicide layer with little pure-silicon inclusion. This situation is much different from the high-energy (6-MeV) implantation of Ni into silicon, where the NiSi₂ is found to be disrupted by unreacted silicon at a dose of $3 \times 10^{17}/\text{cm}^2$ and the NiSi₂ layer forms at a dose as high

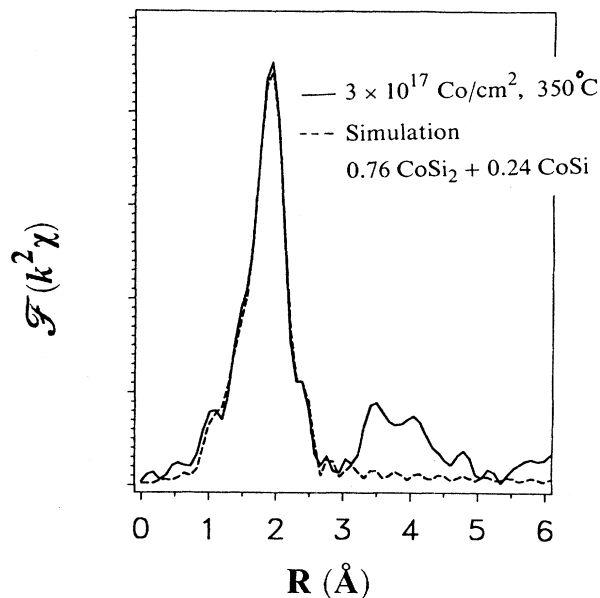


FIG. 3. Fourier-transform magnitude \mathcal{F} of Co EXAFS ($k^2\chi$) for the as-implanted 3×10^{17} -Co/cm² sample and simulation to the first peak with 0.76 (CoSi₂) plus 0.24 (CoSi).

as 1.3×10^{18} Ni/cm² (Ref. 4).

We now turn to the local structure of the samples implanted with high nominal doses; sample *A* with a dose 7.5×10^{17} Co/cm² implanted at 100°C and sample *B* with a dose 8.0×10^{17} Co/cm² implanted at 350°C . Figure 4 shows their Fourier transforms together with the Fe *K*-edge EXAFS of FeSi. FeSi has the same cubic structure as CoSi with a slightly larger lattice parameter (4.49 Å versus 4.46 Å) and is used here to represent the CoSi structure. The near-neighbor shells of sample *A* and sample *B* are analyzed up to 4.0 Å from the Co absorber. The third and fourth shells are analyzed after subtracting out the Co second shell. The peaks between 1.0 and 3.0 Å fit excellently to a Si shell plus a Co shell. The parameters obtained from fitting together with those of bulk CoSi are listed in Table I.

The structures of sample *A* and sample *B* are similar, so the following results apply to both of them. All observed near-neighbor distances (see Table I) from the Co atom in the implanted samples correspond to those of CoSi. The more distant shells of samples *A* and *B* are similar to those of FeSi as seen in Fig. 4. However, the three Si atoms at 2.47 Å expected in the CoSi structure are totally missing in the implanted samples. Further support to this result is gained by examining the envelope functions obtained from the inverse transform of the portion in the 1.0–2.2-Å region (Fig. 4) of the implanted samples and FeSi. The FeSi envelope shows a strong beat characteristic of the two Si shell contribution; in contrast, the implanted samples show no such beat and resemble closely the single-shell Si contribution in CoSi₂.

There are about eight Si atoms observed at 2.34–2.36 Å instead of four Si (one at 2.29 Å and three at 2.33 Å) in the CoSi structure. The coordination numbers obtained

TABLE I. Structural parameters obtained by fitting the Co *K*-edge EXAFS spectra at 77 K of as-implanted samples. Sample *A*: $E=150$ keV, $T_i=100^\circ\text{C}$, dose of 7.5×10^{17} Co/cm². Sample *B*: $E=150$ keV, $T_i=350^\circ\text{C}$, dose of 8.0×10^{17} Co/cm². $\Delta\sigma^2$ is in units of 10^{-3} Å². The numbers in the parentheses are the uncertainties of the last digit(s). The quoted uncertainties are determined by the criterion of double-minimum residue ($2\chi^2$, Ref. 16); for N and σ^2 they are further multiplied by a somewhat arbitrary factor of 2 to take into account the strong correlation among N 's and σ^2 's in the fitting.

Atom	N	Sample <i>A</i>		N	Sample <i>B</i>		CoSi (RT)	
		R (Å)	$\Delta\sigma^2$		R (Å)	$\Delta\sigma^2$		
Si	7.5(8)	2.34(1)	2.6(1.5)	8.2(1.4)	2.36(2)	2.9(2.2)	Si	1 2.287
							Si	3 2.331
							Si	3 2.471
Co	3.0(3)	2.74(1)	-5.1(5)	3.1(4)	2.74(2)	-6.4(6)	Co	6 2.729
Si		3.6 (1)			3.6 (1)		Si	3 3.641
Co		4.00(2)			4.04(2)		Co	6 4.019

in EXAFS here are not affected by any polarization effect if the samples contain either or both of CoSi₂ and CoSi. The observed number of Co atoms at 2.74 Å is about three, which is significantly less than the six expected in a CoSi structure. Note that the effect of the inelastic loss is small for this second shell since R_2 differs from R_1 by only 0.4 Å. If the silicide is uniform in the implanted region, the missing Co atoms may suggest a Si concentration richer than that of CoSi; results from RBS data (Fig. 1) show the Si concentration to be 55%. Sample *A* and sample *B* resemble in general, but differ in detail from the CoSi structure. The nearest-Si-neighbor configuration is more like the eight Si at 2.32 Å in the CoSi₂ structure than that in CoSi, a point to be emphasized further. Other ordered silicide phases such as Co₂Si and CoSi₂ are excluded. The number of isolated Co atoms in the unreacted Si matrix is also small. The local order around the Co atom is of short-range nature

since no diffraction peak (except a very weak one) associated with cobalt silicides was observed. This local order is to be discussed in more detail in the following section.

IV. DISCUSSION

We discuss the silicide formation in the implanted samples in terms of the related silicide structures. It is interesting to observe that a short-range ordered CoSi₂ phase is readily formed in the as-implanted 1×10^{17} Co/cm² sample. The peak Co concentration (12%) at this dose is much less than the stoichiometry of CoSi₂, and the observed CoSi₂ phase does not appear to be Co poor. It is very likely that the CoSi₂ clusters are isolated in the mostly unreacted silicon host.

One feature that persists through the entire dose range of $(1-8)\times 10^{17}$ /cm² is that the Co atom is coordinated with eight Si, i.e., the existence of a (CoSi₈) core. The (CoSi₈) core seems to be highly stable against implantation damage. We speculate that this core forms at doses even lower than 1×10^{17} Co/cm² and acts as a nucleation center for CoSi₂ growth. In an EXAFS study of Fe implanted into silicon with doses of 1×10^{15} to 5×10^{16} Fe/cm², Bunker¹⁷ has found that Fe occupies the interstitial site in silicon and that the first shell around Fe expands while the second shell contracts. In view of his results, the Co implantation may share the same mechanism by Co occupation of the interstitial site in silicon at low doses. As the dose increases, Co atoms may pull the second-shell Si atoms toward the first shell to form the (CoSi₈) core, leaving behind or emitting two extra Si atoms (there are four Si in the first shell and six in the second).

As the implant dose increases, the CoSi₂ clusters grow and become long-range ordered because of greater Co-atom supply. In the meantime, a silicide of Co concentration higher than CoSi₂ starts to form in regions with Co atoms in excess of that for CoSi₂. CoSi is indeed detected in addition to the majority CoSi₂ phase in the as-implanted 3×10^{17} -Co/cm² sample. The total Co retention increases rather slowly as the dose is further increased; the implantation probably creates a large amount of damage to the ordered CoSi and CoSi₂ structures. However, the (CoSi₈) cores seem to remain intact

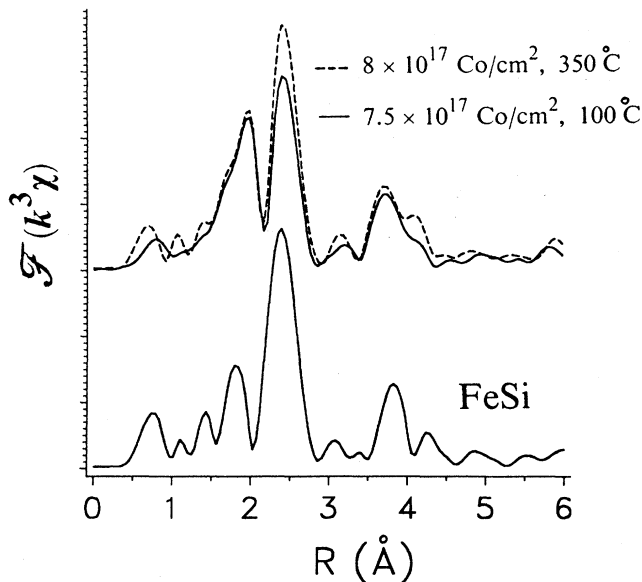


FIG. 4. Fourier-transform magnitude \mathcal{F} of Co EXAFS ($k^3\chi$) for two as-implanted samples and Fe EXAFS of FeSi (lower part). The implant dose and implantation temperature are indicated. All EXAFS data were taken at 77 K.

even if the ordered CoSi_2 is destroyed.

The structure observed in samples *A* and *B* appears to be an intermediate structure between CoSi_2 and CoSi . We propose a mechanism of structural transformation as follows for implantation after the formation of long-range ordered CoSi_2 . The unit cell of CoSi_2 (Fig. 5) consists of a face-centered-cubic Co lattice with a smaller simple cube of eight Si in the interior. This Si cube (shown by dashed lines) has just enough space to accommodate a Co atom at its center with a Co-Si distance of 2.32 Å. The further implanted Co preferentially enters the Si cube in the CoSi_2 formed at doses around $3 \times 10^{17}/\text{cm}^2$. This interstitial Co atom will have eight Si near neighbor (NN) at a single distance of 2.32 Å, as those Co in CoSi_2 already do. The Co atoms in CoSi_2 , which previously had no Co NN at 2.68 Å, now have six or less Co NN at 2.68 Å depending on whether the Si cubes are all filled or not. In samples *A* and *B* only part of the Si cubes can be filled, since the observed Co concentration (44%) is less than the 50% required for full filling. Partial filling of the Si cubes leads to an average number of Co NN at 2.68 Å less than six. Therefore, with a slight lattice expansion the proposed model of Co atom filling of the Si cubes explains satisfactorily the observed first- and second-NN configuration in samples *A* and *B*, namely eight Si at 2.34 Å and three Co at 2.74 Å. Since coordination numbers of the more distant shells cannot be accurately determined, and moreover, the observed NN configuration is only of short-range order, we intend to use our model to understand only the nearest-neighbor shells. The CoSi_2 lattice seems to be expanded after the Co filling; a global expansion of this size is not likely to prevail, leading to a short-range ordered structure. Other types of atomic motion must be involved to achieve the observed CoSi -like radial distribution at distant shells.

We discuss briefly the CoSi_2 growth in the annealed samples. During annealing of the $1 \times 10^{17}\text{-Co}/\text{cm}^2$ sample the isolated CoSi_2 clusters may act as nucleation seeds for further CoSi_2 growth and Co atoms diffuse towards the more seeded region, i.e., the region with higher Co concentration. This diffusion was observed in the RBS spectrum of the annealed sample (Fig. 1). For high-dose samples, the Co concentration in the implanted region is higher than that in CoSi_2 and Co diffusion during annealing should play an important role in the CoSi_2 formation. This Co diffusion behavior was clearly observed in the RBS spectra, for example, the annealed $8 \times 10^{17}\text{-Co}/\text{cm}^2$ sample shows a squarelike distribution of Co with a concentration of about 33% (Ref. 12). The (400) orientation of the CoSi_2 should be due to the Si(100) substrate and the close match between the lattice parameters of Si and CoSi_2 (differ by 1.2%).

V. SUMMARY

Using EXAFS, XRD, and RBS together we have determined the short-range and long-range order of silicide phases in the high-dose cobalt-implanted silicon. An

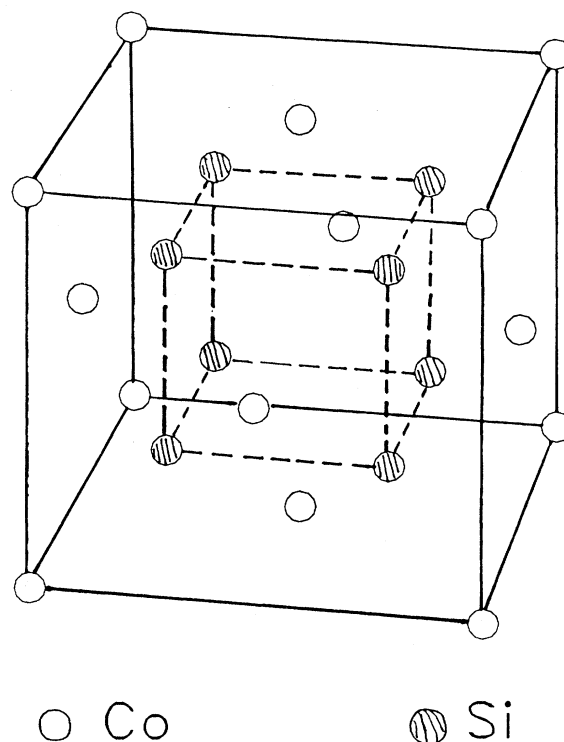


FIG. 5. The unit cell of CoSi_2 . Note the Si cube outlined by dashed lines that has just enough space to accommodate a Co atom at its center.

evolution of short-range ordered CoSi_2 to long-range ordered CoSi_2 and CoSi , and to a defective CoSi -like local order is elucidated. The observed structural evolution enables us to propose a model for the cobalt silicide formation mechanism during implantation. In this model Co atoms preferentially enter the interstitial site, first in silicon, then in CoSi_2 . We have shown the existence of a (CoSi_8) core and its stability against implantation damage, and thus proposed the role of the (CoSi_8) core as a nucleation center in the implanted system.

ACKNOWLEDGMENTS

Z.T. would like to thank Dr. D. M. Pease for helpful discussions. J.I.B. is pleased to thank colleagues at LURE for their hospitality during his stay at LURE in France. We are grateful to LURE for kindly providing beam time and facility support. We acknowledge the support of the U.S. Department of Energy, Division of Materials Sciences, under Contract No. DE-AS05-80ER10742 for its role in development and operation of Beam Line X-11 at the National Synchrotron Light Source. The NSLS is supported by the U.S. Department of Energy (Division of Materials Sciences and Division of Chemical Sciences of the Office of Basic Energy Sciences) under Contract No. DE-AC02-76CH00016.

- *Permanent address: Departamento de Física, Universidad Nacional de La Plata, Casilla de Coreo 67, 1900 La Plata, Buenos Aires, Argentina.
- †Now at SPIRE Corporation, Bedford, Massachusetts.
- ¹F. H. Sanchez, F. Namavar, J. I. Budnick, A. H. Fasihuddin, and H. C. Hayden, in *Beam-Solid Interactions and Phase Transformations*, Vol. 51 of *Materials Research Society Symposium Proceedings*, edited by H. Kurz, G. L. Olson, and J. M. Poate (MRS, Pittsburgh, 1986).
- ²F. Namavar, F. H. Sanchez, J. I. Budnick, A. H. Fasihuddin, and H. C. Hayden, in *Beam-Solid Interactions and Transient Processes*, Vol. 74 of *Materials Research Society Symposium Proceedings*, edited by M. O. Thompson, S. T. Picraux, and J. S. Williams (MRS, Pittsburgh, 1987).
- ³A. E. White, K. T. Short, R. C. Dynes, J. P. Garino, and J. M. Gibson, *Appl. Phys. Lett.* **50**, 95 (1987).
- ⁴J. K. N. Lindner and E. H. te Kaat, *J. Mater. Res.* **3**, 1238 (1988).
- ⁵C. W. T. Bulle-Lieuwma, A. H. van Ommen, and L. van Ijendoorn, *Appl. Phys. Lett.* **54**, 244 (1989).
- ⁶S. P. Murarka, *Silicides for VLSI Applications* (Academic, New York, 1983), p. 30.
- ⁷Reference 6, Chap. IV and references therein.
- ⁸F. A. D'Avitaya, S. Delage, E. Rosencher, and J. Derrien, *J. Vac. Sci. Technol. B* **3**, 770 (1985).
- ⁹F. Namavar, J. I. Budnick, F. H. Sanchez, and F. Otter, *Nucl. Instrum. Methods B* **7/8**, 357 (1985).
- ¹⁰E. A. Stern and S. M. Heald, *Rev. Sci. Instrum.* **50**, 1579 (1979).
- ¹¹G. Tourillon, E. Dartyge, A. Fontaine, M. Lemonnier, and F. Bartol, *Phys. Lett.* **A121**, 251 (1987).
- ¹²Z. Tan, J. I. Budnick, F. Sanchez, G. Tourillon, F. Namavar, H. Hayden, and A. Fasihuddin, in *Synchrotron Radiation in Materials Research*, Vol. 143 of *Materials Research Society Symposium Proceedings*, edited by J. H. Weaver, J. Gland, and R. Clarke (MRS, Pittsburgh, 1989).
- ¹³F. Namavar (unpublished).
- ¹⁴E. A. Stern, B. A. Bunker, and S. M. Heald, *Phys. Rev. B* **21**, 5521 (1980).
- ¹⁵P. A. Lee, P. H. Citrin, P. Eisenberger, and B. M. Kincaid, *Rev. Mod. Phys.* **53**, 769 (1981).
- ¹⁶E.g., P. R. Bevington, *Data Reduction and Error Analysis for the Physical Sciences* (McGraw-Hill, New York, 1969), Chap. 5.
- ¹⁷B. Bunker, *Mater. Res. Soc. Bull. Vol. XIII*, 36 (1988).